Volume 1, Number 1, 13-23, April 2003

International Journal of Vascular Biomedical Engineering

Hemodynamic Characteristics Affecting Restenosis after Percutaneous Transluminal Coronary Angioplasty with Stenting in the Angulated Coronary Stenosis

Byoung Kwon Lee[1¶], Hyuck Moon Kwon[2], Hyung Woon Roh[3], Min Tae Cho[3] and Sang Ho Suh[3]

1 Department of Internal Medicine, College of Medicine, Inje University, Sanggye Paik Hospital
2 Department of Internal Medicine, College of Medicine, Yonsei University
3 Department of Mechanical Engineering, Soongsil University

Abstract

Backgrounds: The present study in angulated coronary stenosis was to evaluate the influence of velocity and wall shear stress (WSS) on coronary atherosclerosis, the changes of hemodynamic indices following coronary stenting, as well as their effect of evolving in-stent restenosis using human in vivo hemodynamic parameters and computed simulation quantitatively and qualitatively. Methods: Initial and follow-up coronary angiographies in the patients with angulated coronary stenosis were performed (n=80). Optimal coronary stenting in angulated coronary stenosis had two models: < 50 % angle changed (model 1, n=43), > 50% angle changed group (model 2, n=37) according to percent change of vascular angle between pre- and post-intracoronary stenting. Flow-velocity wave obtained from in vivo intracoronary Doppler study data was used for in vitro numerical simulation. Spatial and temporal patterns of velocity vector and recirculation area were drawn throughout the selected segment of coronary models. WSS of pre/post-intracoronary stenting were calculated from three-dimensional computer simulation. Results: Follow-up coronary angiogram demonstrated significant difference in the percent of diameter stenosis between two groups (group 1: 40.3±30.2 vs. group 2: 25.5±22.5%, $p<0.05$). Negative WSS area on 3D simulation, which is consistent with re-circulation area of velocity vector, was noted on the inner wall of post-stenotic area before stenting. The negative WSS was disappeared after stenting. High spatial and temporal WSS before stenting fell into within physiologic WSS after stenting. This finding was prominent in Model 2 ($p<0.01$) Conclusions: The present study suggests that hemodynamic forces exerted by pulsatile coronary circulation termed as WSS might affect on the evolution of atherosclerosis within the angulated vascular curvature. Moreover, geometric change, such as angular difference between pre / post-intracoronary stenting might give proper information of optimal hemodynamic charateristics for vascular repair after stenting.

Key words: Wall Shear Stress, In-stent Restenosis, Hemodynamic Analysis, Angulated Coronary Stenosis.

Introduction

The advantages of intracoronary stent over balloon angioplasty include larger acute gains in luminal diameter, and better long-term patency and clinical outcomes[1,2]. Nevertheless, stents provoke greater absolute late luminal loss than balloon angioplasty [3-4] and carry the additional risk of thrombosis[5]. Also, in-stent restenosis has become a current major problem to be solved by interventional cardiologist. Since there are many patient- or lesion-related variables for predicting in-stent restenosis, such as diabetes, unstable angina, reference vessel diameter, final minimum lumen diameter, diameter stenosis, vessel size and lesion length 6, better understanding of biomechanical and biological contributors to in-stent restenosis is important.

¶ 761-7, Sanggye7 dong Nowon-gu, Seoul, 139-707, Korea
E-mail : cardiobk@sanggyebaik.ac.kr

Intimal hyperplasia, which is a main contributor of in-stent restenosis, is occurred from cellular response to vascular injury. The acute cellular response mainly comes from strut-imposed-vascular damage, which dictates the extent of intimal thickening in experimental animals[7,8]. Furthermore, as stent deployment transfixes the artery in a permanently altered shape, the transitions in diameter, contour, and changes of flow pattern may influence on vascular repair and restenosis[9]. Recently, Garasic et al[10] reported that immediate post-deployment luminal geometry determines neointimal thickness independently. When it comes to saying in-stent restenosis there are not only biological but also biomechanical factors to remind. We hypothesized that restenosis of mechanically revascularized coronary arteries by stent may be related in part to abnormalities of disturbed local blood flow and wall shear stress(WSS).

To test the hypothesis that geometrical change of coronary artery after stenting affects on the restenosis by hemodynamic characteristics, such as velocity and WSS, we analyzed the influence of velocity and WSS before and after stenting using human in vivo hemodynamic parameters and in vitro numerical analysis of coronary circulation qualitatively and qualitatively. We also evaluated clinical results of the patients treated with stenting in angulated coronary stenosis.

Materials and Methods

Coronary angiography and stenting in angulated coronary stenosis

Coronary angiography and percutaneous transluminal coronary angioplasty(PTCA) with stenting were performed by the femoral approach according to standard techniques. The coronary lesions with the angulated stenosis (> diameter stenosis of 70%) were selected for PTCA and stenting. Six-month follow up coronary angiography for the evaluation of restenosis was performed (n=80). Each arterial diameter was measured by quantitative coronary assessment (QCA) for percent diameter stenosis. For the delineation of the angulated coronary stenosis, the angular measurements were performed using the serial images of angiography taken in different angle. The highest angulation in stenotic lesion at most longitudinal axis for that artery was chosen for pre-intracoronary stenting angulations. After stenting and six-month follow up coronary angiogram, the corresponding image taken with the same view was used for the measurement of post-intracoronary stenting angulation.

Patient grouping and coronary artery models

Included patients were divided as group for comparing clinical data, and coronary artery models were divided as model based on patient's group for comparing computational hemodynamic characteristics. To evaluate the hemodynamic variables in human coronary models, the basic models were adopted from the measurement of in vivo left coronary artery angiography (Figure 1). For computed simulation, arterial diameter was measured by QCA. And In vivo hemodynamic data of coronary flow including velocity and pressure at proximal and distal regions of interest of coronary artery, which were used for numerical simulation and boundary conditions in this study, were collected by Doppler ultrasound technique by using a 3.5 MHz transducer (Cardiometrics, California, USA) and pressure wire with a 0.014 inch guide wire-mounted pressure sensor (Radi Medical Systems AB, Uppsala, Sweden). Measured physiologic waveforms of the pulsatile coronary blood flow are shown in Figure 2. According to the percent change of vascular angle between pre/post- intracoronary stenting, the patients were divided into two groups: Group 1 (n=43) and model 1: < 50% angle changed, Group 2 (n=37) and model 2: > 50% angle changed (Table 1).

Statistical analysis

Results are expressed as mean ± SD unless otherwise stated. The main statistical analysis of clinical characteristics and angiographic follow up results in 6-month coronary angiography were analyzed by t-test and ANOVA. Comparing WSS before and after

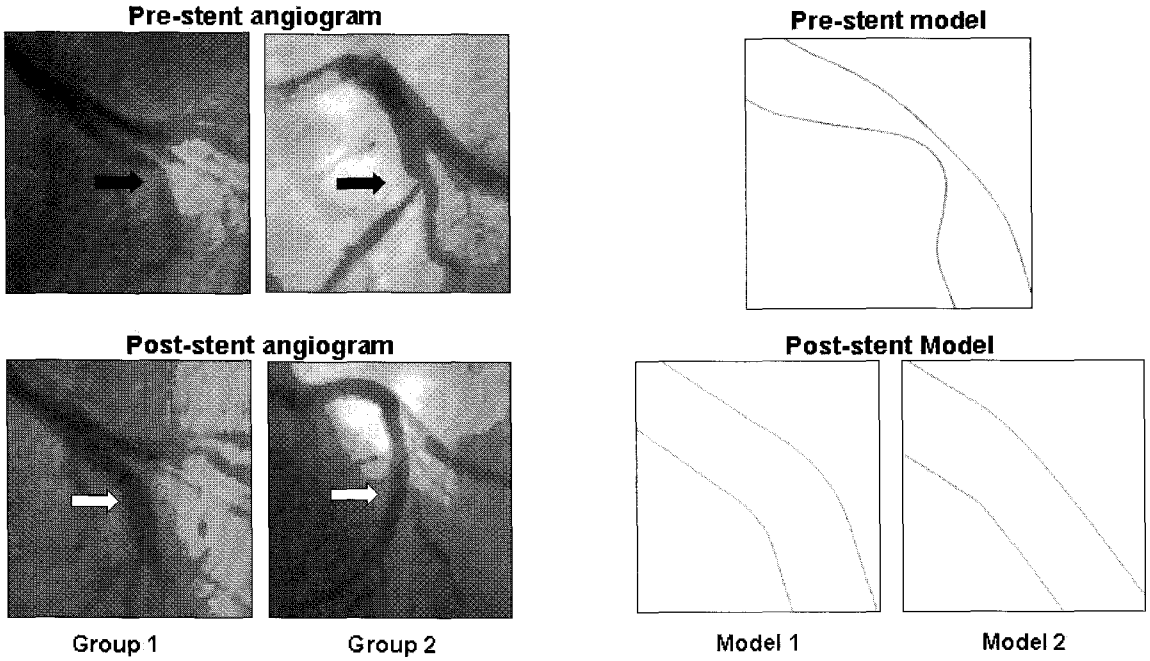

Figure 1 Coronary groups and computerized schematic models before and after stenting, based on the images of human left anterior descending (LAD) artery (Closed arrow: pre-stent stenosis, Open arrow: post-stent). Subjects & Models were grouped by % angle changed (Group & Model 1; <50%, Group & Model 2; >50%).

Table 1 Clinical characteristics of both angulated stent groups.

	Group 1 (n=43)	Group 2 (n=37)	p
Age	58.5±9.9	59.9±10.9	NS
Male (%)	18 (54.5)	18 (66.7)	NS
* LAD/LCX/RCA	22/9/12	17/10/10	NS
Risk factors (%)			
Diabetes M	10 (23.3)	8 (21.6)	NS
Hypertension	19 (44.2)	17(45.5)	NS
Hyperlipidemia	13(30.2)	10(22,0)	NS
Smoking	17 (39.5)	13 (35.1)	NS

* LAD; left anterior descending artery, LCX; left circumplex artery, RCA; right coronary artery Data are presented as mean SD or patient numbers and percentages in parentheses

stenting and WSS of two models were performed by paired and unpaired t-test, respectively.

Numerical analysis of hemodynamic characteristics

1. Governing and Constitutive Equations

The following continuity and momentum equations are used for the computer simulation in order to under blood flow phenomena[11,13].

$$\frac{\partial u_j}{\partial x_j} = 0 \qquad (1)$$

$$\rho\left(\frac{\partial u_i}{\partial t} + u_j\frac{\partial u_i}{\partial x_j}\right) = -\frac{\partial p}{\partial x_i} + \eta\frac{\partial}{\partial x_j}\left(\frac{\partial u_i}{\partial x_j} + \frac{\partial u_j}{\partial x_i}\right) \qquad (2)$$

where ρ, u_i, p, and η are density, velocity vector, pressure, and apparent viscosity, respectively.

2. Treatment of boundary conditions

For the computed simulation calculation, we measured each arterial diameter using a quantitative coronary assessment (QCA) method. We also performed intracoronary two-dimensional ultrasound to measure the vessel wall area, and the luminal areas. Doppler

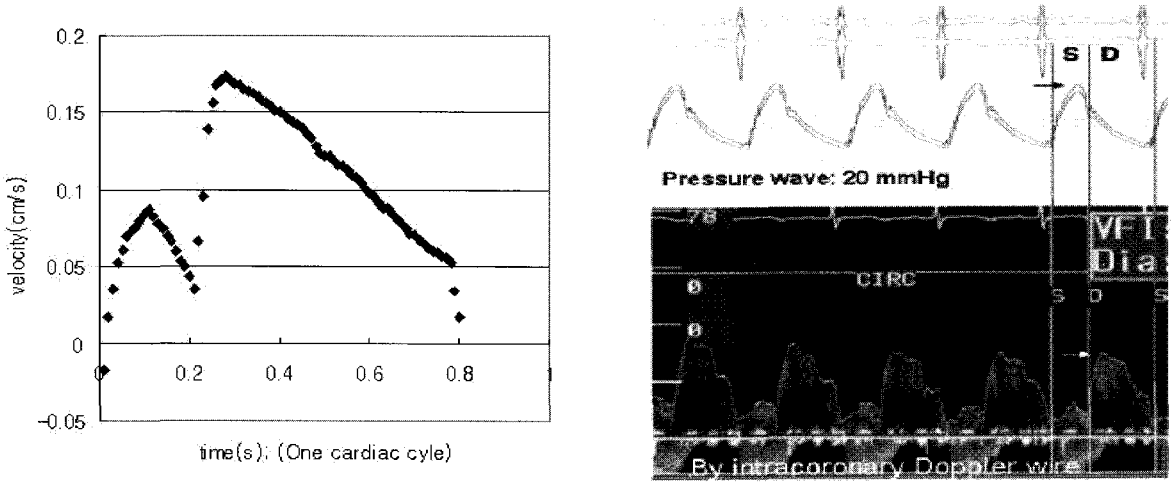

(a) Coronary blood flow model (b) Pressure and Doppler tracing

Figure 2 Physiologic waveform of pulsatile coronary blood flow-velocity model(a) adopted from normal human coronary pressure and Doppler study(b).

ultrasound measurements of the coronary flow-velocity at the proximal and distal regions of interest in the coronary artery were also taken and recorded. During coronary angiography, coronary pressures were simultaneously measured using a guiding catheter and pressure wire (Figure 2)

3. Blood as non-Newtonian fluids

To take into account the rheological characteristics of blood, one has to employ a constitutive equation that represents the apparent viscosity of blood as a function of shear rate. The Carreau model of equation (3) is one of various constitutive equations to specify the apparent viscosity of blood and non-Newtonian fluids[11-12].

$$\eta = \eta_\infty + (\eta_o - \eta_\infty)[1 + (\lambda\dot{\gamma})^2]^{\frac{(q-1)}{2}} \quad (3)$$

where denotes the shear rate. and are the apparent viscosity at infinite-shear-rate and zero-shear-rate, respectively. λ and q represent the characteristic time and index of this model, respectively. As the local shear rate in the flow field is calculated, the apparent viscosity of a non-Newtonian fluid can be determined by Eq. (3). The rheological values of blood as a non-Newtonian fluid are taken to be η_0 =0.056Pa·s, η_∞=0.00345Pa·s, λ=3.313s, and q=0.356 based on the experimental results reported in the literature. The apparent viscosity of blood as a function of the shear rate

4. Numerical method and computational aspects

The distributions of velocity and shear stress of blood flow in the coronary artery are obtained by solving the governing equations. The governing equations are discretized with non-staggered grid systems using the finite volume method. In the non-staggered grid system, the velocity components such as u, v, and w in the momentum equations are calculated for the same points that lie on the grid points of the pressure. This grid system not only simplifies the discretization equations but also efficiently reduces the memory spaces required for computation. However, it may bring out a chequerboard oscillation in the calculation of the pressure field. The oscillating problem is removed by adopting the Rhie-Chow algorithm[13]. This hybrid scheme is adopted for discretization of the convective term and the SIMPLE algorithm for treating the pressure term in the governing momentum equations. The complete matrix is then solved using Stone's method. The fully implicit scheme is used to solve the physiological flow problem, where the time step is set to be 0.01 second. For effective numerical analysis of hemodynamics, we computed with CFX 4 package program (AEA technology, Harwell, UK) in SUN SPARC station 20 (Sun Korea Co., Seoul, Korea).

Table 2 Initial angiographic characteristics

	Group 1 (n=43)	Group 2 (n=37)	p
Balloon data			
Balloon to artery ratio	0.84±0.12	0.83±0.13	NS
Maximal balloon pressure	10.8±1.4	10.9±1.5	NS
Stent data			
Stent diameter(mm)	3.2±0.4	3.1±0.4	NS
Stent length(mm)	23.0±6.6	20.9±6.7	NS
Quantitative coronary angiographic data			
* MLD prestent	0.7±0.3	0.7±0.2	NS
poststent(mm)	3.0±0.3	3.0±0.5	NS
Reference diameter(mm)	3.1±0.3	3.0±0.5	NS
%**DS prestent	78.1±9.3	78.7±8.7	NS
poststent	3.8±4.8	3.2±5.0	NS
Lesion length(mm)	14.5±7.3	13.2±4.1	NS
Vessel angulation (°)			
Vessel angle prestent	43.3±22.5	34.3±22.0	NS
poststent	32.9±19.3	14.7±13.8	<0.001
Changes in angle	10.4±7.0	22.3±13.7	<0.001

* MLD; minimal lesion diameter, **DS; diameter stenosis
Data are presented as mean SD or patient numbers and percentages in parentheses

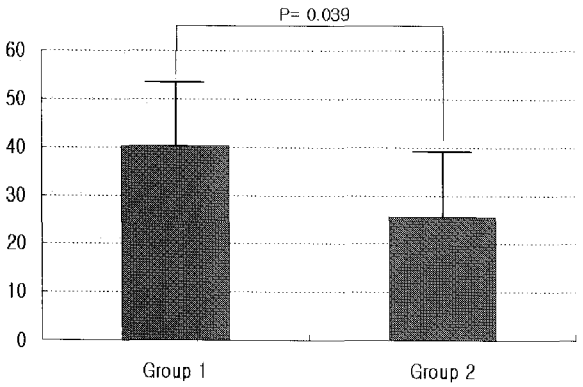

Figure 3. Percent diameter restenosis in 6-month follow up coronary angiography revealed group 2 had significantly lower % of in-stent restenosis than group 1 (p=0.039).

Results

1. Clinical and angiographic results of the patients treated with stenting in angulated coronary stenosis (Table 1-2, Figure 3)

Eighty cases in the patients with angulated coronary stenosis enrolled in this study. Initial clinical characteristics and angiographic findings were not statistically different in both groups (Table 1, 2). So, included cases were well randomized to both groups. Angiographic data before stenting revealed no statistical difference of group 1 and group 2 in balloon to artery ratio, ballooning time, maximal ballooning pressure, stent diameter, stent length, minimal luminal diameter (MLD), reference diameter, % diameter stenosis, and lesion length. However, after stenting, vascular angulation of group 2 (14.7 ± 13.8^0) was statistically smaller than group 1 (32.9 ± 19.3^0)(Table 2).

The clinical outcome both groups was compared with percent diameter stenosis. Percent diameter stenosis in 6-month follow up coronary angiography revealed that group 1 had more severe restenosis rate (40.3 ± 30.2%) than group 1(25.5 ± 22.5%)(Figure 3).

2. Velocity vector change in both coronary artery models before and after stenting (Figure 4).

The velocity vector of pre-intracoronary stenting revealed very high velocity toward outer wall of the artery due to critical coronary stenosis and flow separation, flow recirculation, as well as flow attachment phenomenon nearby the inner wall (Figure 4a). Both post-intracoronary stenting models revealed reduced peak velocity and disappeared flow recirculation in the same coronary artery. This finding was prominent in Model 2 ($p<0.01$)(Figures 4b, 4c)

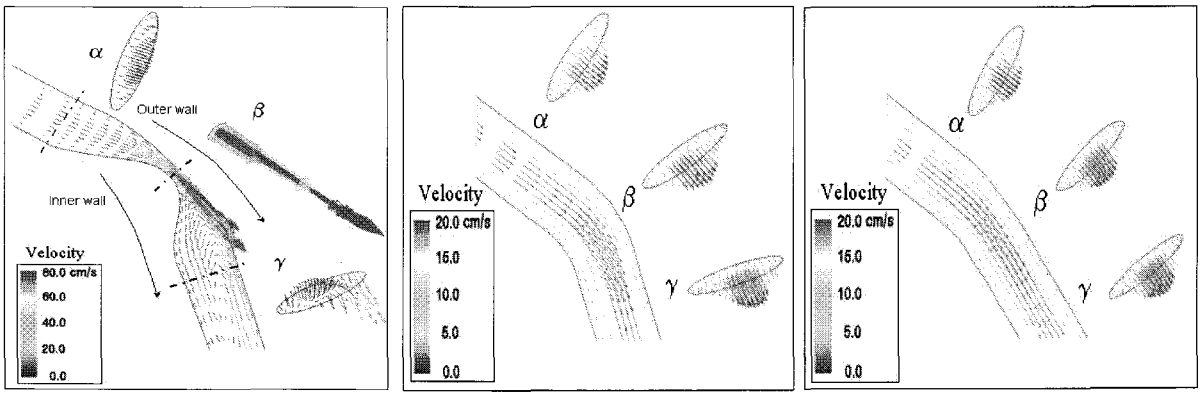

(a) Pre-stent (b) Post-stent: Model 1 (c) Post-stent: Model2

Figure 4 The calculated flow-velocity vectors in pre-, & post-intracoronary stenting models. The flow-velocity vectors revealed very high flow velocity toward outer wall of the artery due to critical coronary stenosis (β) and flow separation, flow recirculation, as well as flow attachment phenomenon at post-stenosed site (γ) in inner wall of pre-stenting model (a). It revealed reduced peak flow velocity and disappeared flow recirculation in the both post-intracoronary stenting models (b, c). This finding was prominent in Model 2.

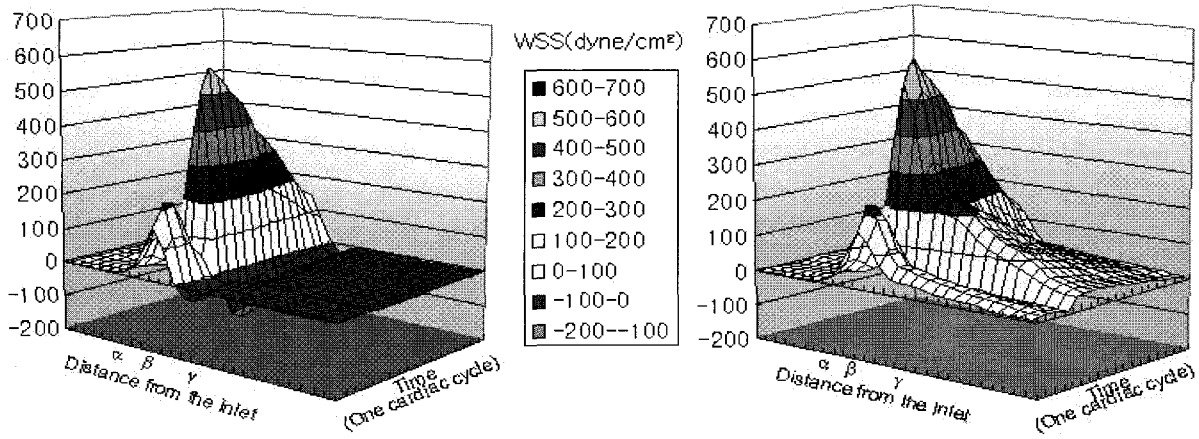

(a) Inner wall (b) outer wall

Figure 5 The 3D shear stress distribution curves in the inner and outer wall of pre-intracoronary stenting model according to time and distance. It revealed the peak shear stress in early diastolic phase, negative shear area in just distal of the highest shear, which is consistent with the recirculation area in inner wall. In the outer wall before stenting, there was also very high shear area similar to inner wall but no negative shear area.

3. Comparison of WSS profiles between both coronary artery models before and after stenting (Figures 5-7).

The 3D spatial and temporal WSS distributions were analyzed, before (Figure 5) and after stenting (Figures 6, 7) according to distance, which means from inlet to outlet of stenotic region and to time, which means from systolic to diastolic phase. Before stenting, it revealed that the development of the peak WSS was in early diastolic phase, negative WSS area was noted around the just distal area of the highest WSS, which is consistent with the recirculation area in inner wall. In the outer wall before stenting, there were also very high WSS area similar to inner wall but no negative WSS area (Figures 5, 6a).

The mean and standard deviation of WSS before and after stenting of two models were drawn in the same chart in each wall (Figures 6, 7). Post-intracoronary stenting WSS showed markedly reduced peak WSS up to about one twentithes comparing with pre- intracoronary stenting WSS in inner and outer wall, as well as disappeared negative WSS area in inner wall (Figures 6b, 6c). It revealed that wide variation of WSS along the fluctuation time and the distance, which means various fluctuation of WSS or oscillatory WSS, was always observed in pre-intracoronary stenting model, and that the variety of WSS was markedly

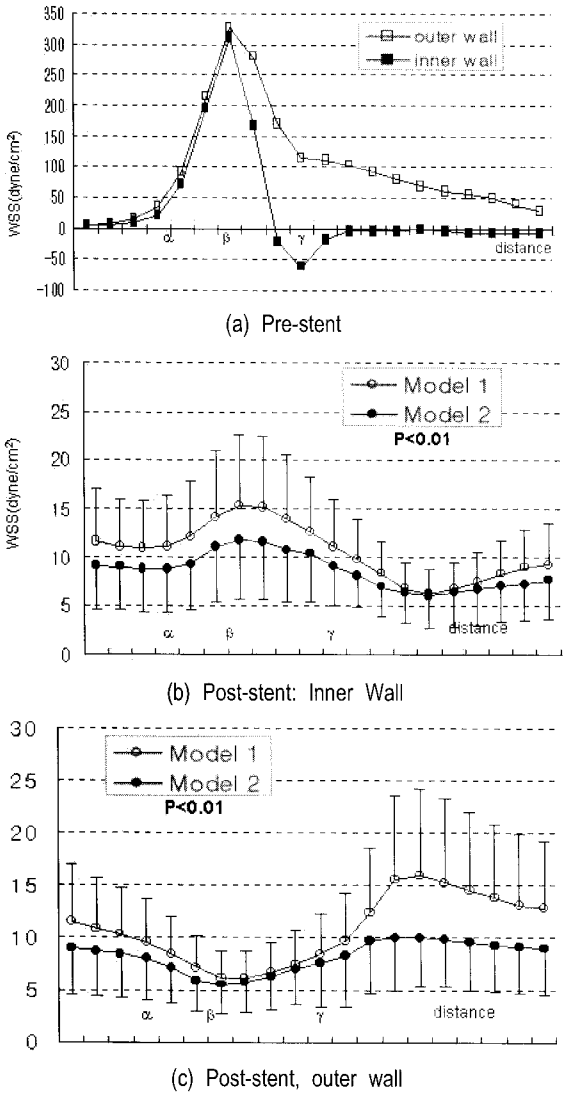

Figure 6 The spatial WSS distribution curve in the inner and outer wall.

Pre- (a) and post-intracoronary stenting (b, c) models along the distance after averaging time factor. Post-intracoronary stenting WSS distribution curve (b, c) showed markedly reduced peak shear stress in both inner and outer wall and disappeared negative shear area in inner wall, while negative shear in pre-stent inner wall. This finding was more prominent in Model 2, and the of waveform of WSS in Model 2 revealed much smaller variation of its amplitude of oscillatory WSS than in Model 1($p<0.01$) along the coronary artery wall.

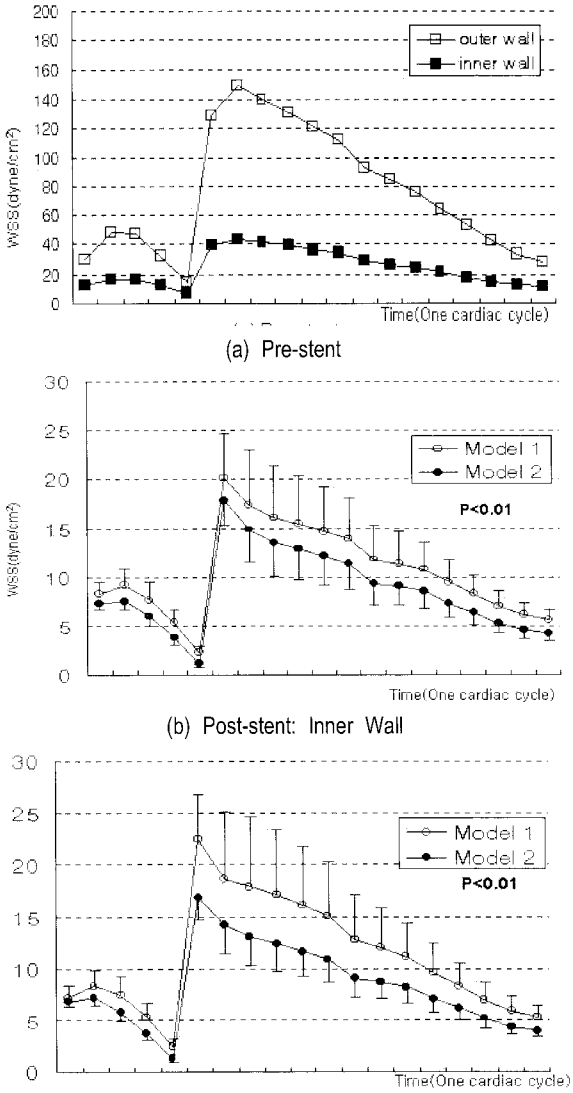

Figure 7 The WSS distribution curve in the inner and outer wall.

Pre- (a) and post-intracoronary stenting (b, c) models after averaging distance factor according to time during one cardiac cycle. Distribution of post- intracoronary stenting WSS (b, c) showed markedly reduced peak shear stress in both inner and outer wall. This finding was more prominent in Model 2, and the of waveform of WSS in Model 2 revealed much smaller variation of its amplitude of oscillatory WSS than in Model 1($p<0.01$) during one cardiac cycle.

diminished in both post-intracoronary stenting model. Furthermore, the waveform of WSS in model 2 revealed much smaller variation of its amplitude than in model 1($p<0.01$) along the coronary artery wall (Figures 6b, 6c) and along the time (Figures 7b, 7c).

Discussion

The present study has extended the understanding of hemodynamic characteristics of pulsatile velocity and WSS conditions at angulated coronary atherosclerotic stenosis and mechanical revascularization with intracoronary stenting after previous study in normal physiologic coronary and aortic circulation[12,14]. Furthermore, we visualized and quantified geometrical patterns of hemodynamic variables in the angulated coronary stenosis models before and after intracoronary stenting, and compared the hemodynamic characteristics

of two models to evaluate in-stent restenosis by in vitro computerized simulation with using in vivo hemodynamic data.

In 6-month follow up coronary angiogram, it revealed that group 2 has lower percent of in-stent restenosis than group 1, which implies the more straightened angle, the less in-stent restenosis rate. This finding supported that the changes of velocity and WSS distributions around the stenotic lesion, which were induced by geometrical changes, might affect on the in-stent restenosis. The velocity vector of pre-intracoronary stenting revealed very high velocity toward outer wall of the artery due to critical coronary stenosis. Flow recirculation nearby the inner wall was also noted. Negative WSS zone, which is consistent with re-circulation area, was noted on the inner wall of post-stenotic area before stenting, and this finding was more prominent than non-stenotic normal coronary artery[12,14]. And, this negative WSS area was disappeared after intracoronary stenting. The WSS after stenting was markedly reduced up to about one twentieths from that of before stenting. The amplitude of WSS fluctuation in model 1 of post-intracoronary stenting was significantly larger than that in model 2. The six-month in-stent restenosis was higher in group 1 represented model 1. The present study suggested that hemodynamic forces exerted by flowing blood termed WSS might affect on the evolution and progression of atherosclerosis within the angulated vascular curvature. Furthermore, this study demonstrated that geometric characteristics, such as angular difference between pre- and post-intracoronary stenting might affect vascular repairing associated with hemodynamic characteristics.

Endothelial cells are exposed to the blood flow, and as a result, the cells can be chronically exposed to shear forces with cyclical variation in direction 15. It was reported that the recirculation area with low WSS area might contribute to the atherogenesis and progression of atherosclerosis[12,14,16]. As described above, the flow disturbances occurred prominently on the curved inner wall after stenosis. Therefore, the atherosclerosis might initiate and progress on the inner wall of a curve due to low velocity, flow separation, flow recirculation and low WSS. Forces exerted by flow disturbances flowing on the vascular endothelium has been also implicated in the vascular remodeling after percutaneous transluminal balloon angioplasty or coronary stenting[17] Also, this insight provided the basis for the rational design of coronary arterial bypass surgery[18].

Since there are many variables for predicting in-stent restenosis, we would like to investigate the effect of biomechanical factors to restenosis. The endothelial lining has a dynamically mutable interface, local responsiveness to various stimuli originating from the circulating blood and/or neighboring cells and tissues, and thus can actively participate in the physiological adaptation or pathophysiological dysfunction of a given region of the vasculature[19-20]. Biomechanical modulation of endothelial gene expression, in particular, the genes encoding positive and negative WSS responsive elements in the promoters of biomechanically responsive genes and adhesion molecules involved in cell-cell and cell-matrix interactions, may also play an active role at times of hemodynamic transitions such as percutaneous transluminal coronary angioplasty or stenting[19]. Laminar WSS stimulates expression of tissue plasminogen activator and reduces secretion of plasminogen activator inhibitor type-1. Importantly, endothelial cells exposed to turbulent flow failed to show increases in thrombomodulin and tissue plasminogen activator, which means prothrombotic condition[21-22]. During first several hours after stenting when thrombosis occurs predominantly, if sustained disturbed WSS in the stented region exists, it might stimulate more thrombosis. After then, as platelets in the thrombus secrete various growth factors, the proliferation will occur much more leading to in-stent restenosis. The present study demonstrated that significant temporal and spatial WSS fluctuation in post-intracoronary stenting status was still remained in model 1, represented group 1, and there was the higher percent of diameter stenosis at follow-up angiography. This result may indicate the adverse effect of remaining WSS fluctuation on the healing process after stenting. Therefore, we might assume that if

there are distinct biomechanical factors for the progression of atherosclerosis or in-stent restenosis, such as low WSS or temporally disturbed WSS fluctuation, there will be more cellular proliferation during early healing period in the stented coronary vasculature.

WSS affects on various biological cascades, and it may be critical for endothelial cell survival[15]. Davies et al. demonstrated increased endothelial cell turn over in areas that experience turbulent WSS condition, suggesting compromised endothelial cell integrity under these conditions[23]. It has been also reported that the lack of WSS triggers apoptosis in endothelial cells[24]. Mechanically, physiological levels of WSS interfere with numerous steps of the endothelial cell apoptotic cascade. Sustained physiological levels of WSS activate the P13K/Akt pathway in an integrin-dependent fashion, thereby mimicking the signaling pathways used by specific endothelial cell growth factors such as VEGF or Ang-1[25]. Under low WSS condition, endothelial cells on the border of a wound edge failed to maintain contact with neighboring cells and were oriented randomly. Further, cells spread and migrate into wound sits more slowly[26]. And, Charles et al also reported that the temporal WSS gradient stimulates endothelial cell proliferation, based on their experimental result[27].

Therefore, we suggest that vascular endothelial cells might be influenced by local WSS condition in re-endothelialization period after PTCA or stenting. The stented coronary artery having disturbed and WSS fluctuation due to its geometric alteration, complete endothelialization might be delayed with dysfunctional endothelial cells. It results in longer exposure time of subendothelium to various growth factors and cytokines causing more intimal hyperplasia. In this study, although the post-stented WSS of both inner and outer wall in both models was in lower margin of physiologic WSS level, the less straightened model 1 had significant amount of temporal and spatial WSS fluctuation. The WSS variation in model 2 was significantly small in physiologic WSS range. Therefore, the lower percent diameter stenosis in group 2, represented model 2, also could be inferred.

In spite of new findings described above, there are some limitations in this study. At first, the in-stent restenosis occurs with so many factors that we cannot say that hemodynamic characteristics at stented lesion mainly take the responsibility of restenosis. Another is that the straightening effect itself is biologically stressful for nature vessels. We did not evaluate biologic consequences of this effect in vivo. We just suggest a physiologic role of hemodynamic variables after geometric change by hemodynamic analysis methods to vascular healing process after percutaneous coronary intervention with stent with clinical data. It will be needed further experiments under various in vitro and in vivo conditions with larger scale clinical data of in-stent restenosis.

Finally, these results may be used in coronary intervention to prevent the restenosis of coronary arterial disease and the progression of itself. Future investigations on the biomechanical activation of endothelial cells would be a conceptually rich in this pathophysiologically relevant area.

Acknowledgement

This work was supported by grant No. R01-2002-000-00561-0(2002) from Basic Research Program of the Korea Science & Engineering Foundation.

References

1. Serruys PW. de Jaegere P, Kiemeneij F, Macaya C. Rutsch W, Heyndrickx G, Emanuelsson H. Marco J, Legrand V, Materne P, Belardi J, Sijwart U. Colombo A, Goy J, van den Heuvel P. Delcan J, More M. A comparison of balloon-expandable-stent implantation with balloon angioplasty in patients with coronary artery disease. N Engl J Med. 1994;331:489-495.
2. Fischman DL. Leon MB, Baim DS. Schatz RA. Savage MP. Penn IM, Detre K, Veltri L. Ricci DR, Nobuyoshi M, Cleman MW, Heuser RR, Almond D, Teirstein PS, Fish RD, Colombo A, Brinker J. Moses J, Shaknovich A. Hirshfeld

J, Bailey S, Ellis S, Rake R, Goldberg S. A randomized comparison of coronary artery-stent placement and balloon angioplasty in the treatment of coronary artery disease. N Engl JMed. 1994; 331:496-501.

3. Kuntz RE, Safian RD. Levine MJ, Reis GJ, Diver DJ. Baim DS. Novel approach to the analysis of restenosis after the use ol three new coronary devices. J Am Coll Cardiol. 1992;19: 1493-1499.
4. Kuntz RE, Gibson CM, Nobuyoshi M, Baim DS. Generalized model of restenosis after conventional balloon angioplasty, stenting, and directional atherectomy. J Am Coll Cardiol. 1993:21:15-25.
5. Hasdai D, Garratt KN, Holmes DR, Berger PB, Schwartz RS, Bell MR. Coronary angioplasty and intracoronary thrombolysis are of limited efficacy in resolving early intracoronary stent thrombosis. J Am Coll Cardiol. 1996:28:361-367.
6. Minz GS, Foffmann R, Mehran R, Pichard AD, Kent KM, Satler LF, Popma JJ, Leon MB. In-stent restesnosis: the Washington Hospital Center experience. Am J Cardiol 1998;81(7A):7E-13E.
7. Schwartz RS, Holmes DH, Topol EJ. The restenosis paradigm revisited. J Am Call Cardiol. 1992; 20:1284-1293.
8. Schwartz RS. Huber KC, Murphy JG, Edwards WD, Camrud AR, Vlietstra RE, Holmes DR. Restenosis and proportional neointimal response to coronary artery injury. J Am Coll Cardiol. 1992;19: 267-274.
9. Edelman ER, Rogers C. Hoop dreams; stent without restenosis. Circulation 1996;94:1199-1202.
10. Garasic JM, Edelman ER, Squire JC, Seifert P, Williams MS, Rogers C. Stent and artery geometry determine intimal thickening indepent of arterial injury. Circulation 2000;101:812-818.
11. Patankar SV. Numerical heat transfer and fluid flow. New York:McGraw-Hill;1980.
12. Lee BK, Kwon HM, Kim D, Yoon YW, Seo JK, Kim IJ, et al. Computed numerical analysis of the biomechanical effects on coronary atherogenesis using human hemodynamic and dimensional variables. Yonsei Med J 1998;39:166-174.
13. Rhie CM, Chow WL. Numerical study of turbulent flow past an airfoil with trailing edge seperation. J Am Instit Aeron Astron 1983;21: 1527-1532.
14. Lee BK, Kwon HM, Hong BK, Park BE, Suh SH, Cho MT, Lee CS, Kim MC, Kim CJ, Yoo SS, Kim HS. Hemodynamic effects on atherosclerosis-prone coronary artery: wall shear stress/rate distribution and impedance phase angle in coronary and aortic circulation. Yonsei Med J 2001;42(4):375-383.
15. Traub O, Berk BC Laminar shear stress: mechanism by which endothelial cells transduce an Atheroprotective force. Arterioscler Thromb Vasc Biol 1998;18:677-685.
16. Malek AM, Alper SL, Izumo S. Hemodynamic shear stress and its role in atherosclerosis. JAMA 1999;282:2035-2042.
17. Van Langenhove G, Wentzel JJ, Kram R, slager CJ, hamburger JN, Surruys PW. Helical velocity patterns in a human coronary artery: A three-dimensional computational fluid dynamic reconstruction showing the relation with local wall thickness. Circulation 2000;103:e22-e26.
18. Kim D, Kwon HM, Lee BK, Jang Y, Suh SH, Yoo SS, Kim HS. Hemodynamic effects of the geometric dimensions of graft vessels in coronary artery bypass graft models. J Kor Med Sci 1998;13:263-268.
19. Gimbrone MA Jr., Nagel T, Topper JN. Perspectives series: cell adhesion in vascular biology; Biomechanical activation: an emerging paradigm in endothelial adhesion biology. J Clin Invest 1997;99:1809-1813.
20. Konstantopoulos K and McIntire LV. Perspectives series: Cell adhesion in vascular biology; effects of fluid dynamic forces on vascular cell adhesion. J Clin Invest 1996;98:2661-2665.
21. Malek AM, Jackman R, Rosenberg RD, Izumo S. Endothelial expression of thrombomodulin is reversibly regulated by fluid shear stress. Cir Res 1994;74:852-860.
22. Takada Y, Shinkai F, Kondo S, Yamamoto S, Tsuboi H, Korenaga R, Ando J. Fluid shear stress increases the expression of thrombomodulin

by cultured human endothelial cells. Biochem Biophys Res Commun. 1994;205:1345-1352.

23. Davis PF, Remuzzi A, Gordon EJ, Dewey CF jr, Gimgrone MA Jr. Tubulent fluid shear stress induces vascular endothelial cell turnover in vitro. Proc Natl Acad Sci USA 1986;83:2114-2117.
24. Kaiser D, Freyberg MA, Friedl P. Lack of hemodynamic forces triggers apoptosis in vascular endothelial cells. Biochem Biophys Res Commun 1997;231:586-590.
25. Dimmeler S, Assmus B, Hermann C, Haendeler J, Zeiber AM. Fluid shear stress stimulates phosphorylation of Akt in human endothelial cells: involvement in suppression of apoptosis. Circ Res 1998;83:334-342.
26. Vyalov S, Langille BL, Gotlieb AI. Decreased blood flow rate disrupts endothelial repair in vivo. Am J Pathol 1996;149:2107-2118.
27. White CR, Haidekker M, Bao X, Frangos JA. Temporal gradients in shear, but not spatial gradients, stimulate endothelial cell proliferation. Circulation 2001;103:2508-2513.